# A Theoretical Examination of Solvatochromism and Solute-Solvent Structuring in Simple Alkyl Carbonyl Compounds. Simulations Using Statistical Mechanical Free Energy Perturbation Methods

**Stephen E. DeBolt and Peter A. Kollman***

*Contribution from the Department of Pharmaceutical Chemistry, University of California, San Francisco, California 94143.* *Received August 30, 1989*

**Abstract:** With use of the statistical mechanical free energy perturbation method (FEP), the difference in Gibbs free energies ($\Delta\Delta G_s$) and potential energies ($\Delta\Delta V_s$) of solvation for the ground state versus the n → π* excited state were calculated for the carbonyl containing chromophores formaldehyde and acetone. $\Delta\Delta V_s$ corresponds to the difference in excitation energy (ground state to Franck-Condon state transition) for a chromophore in the vapor phase versus when solvated, i.e. the solvent shift energy. $\Delta\Delta G_s$ corresponds to the solvated versus vapor phase energy difference (ground to solvent equilibrated excited state), i.e. the difference in free energy between the two adiabatic states. By the term "solvent equilibrated excited state" we refer to the thermally relaxed, solvent equilibrated system containing the electronically excited solute molecule, where Franck-Condon strain has been alleviated. Results were obtained for the carbonyl solutes in TIP3P water, modified-OPLS methanol, and five-center $CCl_4$ model solvents. Although experimentally measured UV solvent shifts were not quantitatively reproduced in all cases, the calculated difference-energy values exhibited the proper qualitative trend in magnitudes with respect to this series of solvents. The calculated difference-energy values were found to compare particularly well with experimentally observed UV solvent shifts for the n → π* electronic transitions in water and methanol. Characteristics of solute-solvent orientational structuring were examined for both ground- and excited-state solutes, especially in their relationship to solute-solvent interaction energies. Solute-solvent radial distribution functions provide interesting insight into the different characteristics of the average solvent structures around the ground- and excited-state solutes. Intermolecular energy pair distribution functions reported for the ground, the Franck-Condon, and the equilibrated-excited states illustrate a progressive loss of solute-solvent hydrogen bonding and indicate further desolvation of the solute after excitation in polar solvents. The solvent's response upon n → π* solute excitation is consistent with current ideas regarding the solvation of hydrophobic moieties. An examination of the solvent-solvent interactions in the solute near-shell and bulk solvent illuminates how the change in the relative strengths of solvent-solvent versus solute-solvent interactions drives the restructuring of the near-shell solvent cage, thus contributing to the differential solvation of ground- and excited-state solutes.

## Background and Introduction, the n → π* Transition

Solvatochromism refers to the phenomena wherein solvents may affect the position, intensity, and shape of UV absorption (or emission) spectra relative to the vapor phase. Qualitatively, the n → π* transition involves the promotion of an n-electron from the carbonyl oxygen's lone-pair orbital to the empty antibonding π* orbital, which is delocalized over the carbonyl group. This results in an overall reduction of the magnitude of the molecular dipole moment in the excited state.[1,2]

The solvent-dependent shift of the n → π* electronic transition band of carbonyl compounds toward shorter wavelengths in polar solvents is largely due to the differential solvation of the ground versus the excited state of the solute. This has been attributed to factors such as specific interactions, e.g. hydrogen bonding, in hydroxylic solvents, and more generally to solvent dielectric effects such as dipole-dipole and dipole-induced dipole interactions as well as packing and orientation strain in the Franck-Condon excited state. For all of the n → π* transitions considered in this study, the ground-state solute has a larger permanent dipole moment than in the excited state, and it is thus expected to exhibit a more well defined solute-solvent orientation due to stronger interactions in polar solvents. Such solutes are more favorably solvated in their ground state than in their excited state, thereby increasing the energy difference between states. This corresponds to a blue shift of transition frequency in polar solvents.[3-9]

A shift of the carbonyl n → π* band toward longer wavelengths is seen in some nonpolar nonorienting solvents. Bayliss and McRae have attributed this "polarization red shift" to the electronically polarizable solvent's ability to facilitate the formation of the transition moment that develops in the process of absorption or emission.[10a-c] This effect is present in all solvents, but it figures most prominently in the red shift of the carbonyl n → π* bands in such solvents as $CCl_4$, benzene, and alkanes[10c] where orientational polarization is minimal. An alternative contribution to this effect is the decreased stabilization of the ground state relative to the excited state due to more favorable solute-solvent dispersion interactions involving the electronically diffuse excited state.

Ab initio CI calculations of optimally oriented, hydrogen-bonded, formaldehyde-water and acetone-water dimers have given dimerization energies that are nearly equal to the energy of the blue shift of these solutes in bulk water.[11a] Conclusions were drawn from these calculations as to the number of hydrogen bonds that form between these solutes and water. Also, the blue shift was attributed to the energy required to (largely) break the hydrogen bond between a solute's carbonyl oxygen lone-pair orbital and the hydroxyl group of water, a phenomenon that occurs on n → π* electronic transition.

After experimentally determining enthalpies of transfer of ketones and other organic solutes, and coupling these results with spectroscopic information, Haberfield concluded that the above explanation of solvent-induced frequency shifts was overly sim-

(1) Freeman, D. E.; Klemperer, W. *J. Chem. Phys.* **1966**, *45*, 52-57.
(2) Streitwieser, A.; Kohler, B. *J. Am. Chem. Soc.* **1988**, *110*, 3769-3772.
(3) Scheibe, G.; Felger, E.; Rossler, G. *Ber.* **1927**, *60*, 1406.
(4) Barltrop, J. A.; Coyle, J. D. *Excited States in Organic Chemistry*, John Wiley & Sons, Ltd.: New York, 1975; p 60.
(5) Halverson, F.; Hirt, R. C. *J. Chem. Phys.* **1951**, *19*(6), 711-718.
(6) McConnell, H. *J. Chem. Phys.* **1952**, *20*(4), 700-704.
(7) Brealey, G. J.; Kasha, M. *J. Am. Chem. Soc.* **1955**, *77*, 4462-4468.
(8) Pimentel, G. C. *J. Am. Chem. Soc.* **1957**, *79*, 3323-3326.
(9) Krishna, V. G.; Goodman, L. *J. Chem. Phys.* **1960**, *33*(2), 381-386.

(10) (a) Bayliss, N. S. *J. Chem. Phys.* **1950**, *18*(3), 292-296. (b) Bayliss, N. S.; McRae, E. G. *J. Phys. Chem.* **1954**, *58*, 1002,1006. (c) Bayliss, N. S.; McRae, E. G. *J. Phys. Chem.* **1954**, *58*, 1006-1011.
(11) (a) Del Bene, J. E. *J. Chem. Phys. Lett.* **1973**, *23*(2), 287-291. Del Bene, J. E. *J. Am. Chem. Soc.* **1973**, *95*(20), 6517-6522. Del Bene, J. E. *J. Am. Chem. Soc.* **1974**, *96*(17), 5643-5644. Del Bene, J. E. *J. Chem. Phys.* **1975**, *62*(20), 666-669. Del Bene, J. E. *J. Chem. Phys.* **1975**, *63*(11), 4666-4671. (b) Blair, J. T.; Westbrook, J. D.; Levy, R. M.; Krogh-Jespersen, K. *Chem. Phys. Lett.* **1989**, *154*, 531-535.

0002-7863/90/1512-7515$02.50/0 

plistic.[12] It was found that the n → π* blue shift of carbonyl compounds on going to more polar solvents was due only in part to superior solvation of the ground state, but also in significant part to the desolvation of the nonpolar excited state in the polar solvent.

The experimental absorption data for the n → π* transition in formaldehyde and acetone is most representative of the $S_0 \rightarrow S_1$ excitation. $\lambda_{max}$ is in the vicinity of 3400 (formaldehyde) or 2800 (acetone) Å, depending on the solvent and temperature.[13-17] For acetone in several solvents, Borkman and Kearns's experiments have shown that, after excitation to the singlet, rapid intersystem crossing (ISC) to the triplet ($S_1 \rightarrow T_1$) occurs, at a rate that is independent of temperature between 77 and 298 K, and is approximately 100 times the rate of $S_1 \rightarrow S_0$ radiation ($\Phi_{ISC} = 1.0 \pm 0.1$; $k_{ISC} = 4 \times 10^7\ s^{-1}$). This has been shown to account for acetone's measurably low fluorescence quantum yield ($\Phi_F = 0.01 \pm 0.003$) at 25 °C.[17] The lifetime of the lowest n → π* singlet $S_1$ was measured as $\tau_{S1} = 2.5 \times 10^{-8}\ s^{-1}$. This allows plenty of time for the solvent to reorient (which occurs within picoseconds) after excitation, prior to emission.

The intent of this study has been 2-fold: first, to determine how well a molecular dynamics (MD) implementation of the statistical mechanical perturbation methodology, using a two-body interaction potential and a simple electrostatic model for the ground and excited states, can reproduce the solvent dependent frequency shift energies for the well-characterized n → π* electronic transitions of simple alkyl carbonyls, and second, to examine the intermolecular orientational structuring that occurs at room temperature in fluid media between the ground and excited states of these carbonyl solutes and a series of several different solvents spanning the range from polar to nonpolar.

## Methods and Models

All MD calculations were carried out with constant temperature (25 °C for water and methanol, 20 °C for $CCl_4$), constant pressure (1 atm), and composition (single solute) ensembles by coupling to a heat and pressure bath.[18] The original thicknesses of the solvent shells (radius out from the solute) before the application of cubic periodic boundary conditions were (in Å) 10.0 for all simulations in water, using a nonbonded cutoff of 8.0, 14.0 for all simulations in methanol, using a 9.5 cutoff, and 15.0 for all simulations in $CCl_4$, with a 10.0 cutoff. For simulations run in TIP3P water and $CCl_4$ solvents, a molecular dynamics timestep of 2 fs was used (3 fs for formaldehyde in water), and for the methanol simulations a timestep of 1 fs was used. Physically realistic atomic masses were used, e.g. 12.01 for carbon, on all centers. Van der Waals' parameters for the solutes were taken directly from the Wiener et al. all-atom force field.[19]

Molecular geometries and molecular orbital (MO) charge distributions used for the ground- and excited-state solutes formaldehyde and acetone were generated from ab initio calculations with the Gaussian-82 program,[20a] except for the acetone n → π* $S_1$ excited state, for which the optimized geometry and MO electronic distribution were obtained with the GAMESS program.[20b] This corresponds to isolated monomers at 0.0 K at their zeroth vibrational levels. Geometry optimizations of the monomers were at the 6-31G** basis set level for formaldehyde and 6-31G* for acetone. R groups attached to the carbonyl carbon bent out of plane about 40° for both formaldehyde and acetone during excited-state optimization, attaining the well-documented pyramidal structure. Atom-centered point charges were obtained by fitting to the electrostatic potentials generated with the above basis sets with the program G80UCSF,[21a] via the fitting procedure described previously.[21b]

**Table I.** Interaction Potential Parameters

| atom | $Q(S_0)$[b] | $Q(T_1)$ | $Q(S_1)$ | $R^*/2$[c] | $\epsilon$ |
|---|---|---|---|---|---|
| | | Acetone | | | |
| $\mu_{GS} = 3.13_{calc}$, $2.88_{expt}$ D;[a] $\mu_{XS} = 1.77_{calc,T1}$, $1.87_{calc,S1}$ D | | | | | |
| O | −0.5812 | −0.1944 | −0.2114 | 1.60 | 0.20 |
| C | 0.8177 | 0.1482 | 0.1652 | 1.85 | 0.12 |
| methyl C | −0.5252 | −0.3003 | −0.3003 | 1.80 | 0.06 |
| H | 0.1356 | 0.1078 | 0.1078 | 1.54 | 0.01 |
| | | Formaldehyde | | | |
| $\mu_{GS} = 2.66_{calc}$, $2.33_{expt}$ D;[d] $\mu_{XS} = 1.55_{calc,T1}$, $1.29_{expt,T1}$, $1.56_{expt,S1}$ D[e] | | | | | |
| O | −0.4604 | −0.1029 | | 1.60 | 0.20 |
| C | 0.4421 | −0.2674 | | 1.85 | 0.12 |
| H | 0.0091 | 0.1851 | | 1.54 | 0.01 |

| Carbon Tetrachloride | | | | | |
|---|---|---|---|---|---|
| atom | Q(STO-3G) | Q(6-31G*) | $Q(\Omega=15)$[f] | $R^*/2$ | $\epsilon$ |
| C | +0.3560 | −0.5872 | −1.20 | 2.5817 | 0.1017 |
| Cl | −0.0890 | +0.1468 | +0.30 | 1.9900 | 0.2270 |

[a] The experimental ground-state dipole moment value $\mu_{GS}$ (D) is from: Weast, R. C., Ed. *Handbook of Chemistry and Physics*, 55th ed.; CRC Press: Cleveland, 1973. [b] $Q(S_0)$, $Q(T_1)$, and $Q(S_1)$, are atom-centered charges used for the ground state and the excited states, respectively. [c] R* is the van der Waals radius (Å) on the atom, and $\epsilon$ is the van der Waals equilibrium well depth energy (kcal/mol) used in pairwise atom–atom interactions. [d] The experimental ground-state dipole moment value $\mu_{GS}$ from ref 15. [e] The experimental $S_1$ and $T_1$ excited-state dipole moment values are from refs 15 and 16. [f] Charges that reproduce a reasonable octapole moment.[32]

For the molecular dynamics, no attempt was made to explicitly model electronic distributions in terms of directed spatial spin orbitals nor to include differences in ground-state versus excited-state solute van der Waals interaction parameters. Notice (Table I) that while the magnitude of the formaldehyde dipole moment resulting from the ab initio triplet calculation (1.55 D) is closer to that experimentally observed for $S_1$ (1.56 D), the difference in dipole moment magnitudes for ground state versus triplet is well preserved (2.33 − 1.29 = 1.04 D, experiment; 2.66 − 1.55 = 1.11 D, calculated). We will occasionally refer to the π* states modeled in this study as simply "the excited state".

Bond and angle force constants for the molecular mechanical formaldehyde were iteratively least squares fit to reasonably reproduce the known ground-state vibrational frequencies[22] in normal mode calculations. Excited-state force constants were extrapolated from these, e.g. the carbonyl force constant was slightly reduced corresponding to the longer, weaker C–O bond. An "improper" 180° dihedral (e.g. H1–H2–C–O) force constant was used to constrain the formaldehyde and acetone ground states more firmly to the planar configuration. Force constants used for acetone were similar to those in formaldehyde (see Table II).

Three different solvent models were used: (1) TIP3P waters,[23] (2) modified-OPLS methanol[24] composed of three centers H, O, and $CH_3$, where the methyl group is a united atom center, and (3) five-center tetrachloride. All solvents were equilibrated as pure solvents prior to solute insertion and are known (TIP3P water) or were required ($CCl_4$, modified-OPLS methanol) to reproduce experimental heats of vaporization and density to within a few percent. For simulations run in TIP3P water and $CCl_4$ solvents, all solute and solvent bonds were constrained to remain rigid by using SHAKE, an algorithm that permits retention of fixed internal geometries during MD.[25] Simulations run in modi-

(12) Haberfield, P. *J. Am. Chem. Soc.* **1974**, *96*(20), 6526–6527. Haberfield, P.; Lux, M. S.; Rosen, D. *J. Am. Chem. Soc.* **1977**, *99*(21), 6828–6831. Haberfield, P. J.; Rosen, D.; Jasser, I. *J. Am. Chem. Soc.* **1979**, *101*(12), 3196–3199.
(13) (a) Clouthier, D. J.; Ramsay, D. A. *Annu. Rev. Phys. Chem.* **1983**, *34*, 31–58. (b) Turro, N. J. *Modern Molecular Photochemistry*; The Benjamin/Cummings Publishing Co., Inc.: New York, 1978; Chapter 5.
(14) Cohen, A. D.; Reid, C. *J. Chem. Phys.* **1956**, *24*(1), 85–88.
(15) (a) Lombardi, J. R.; Freeman, D. E.; Klemperer, W. J. *J. Chem. Phys.* **1967**, *46*, 2746. (b) Freeman, D. E.; Klemperer, W. J. *J. Chem. Phys.* **1964**, *40*, 604. (c) Freeman, D. E.; Klemperer, W. J. *J. Chem. Phys.* **1966**, *45*(1), 52–57.
(16) Buckingam, A. D.; Ramsay, D. A.; Tyrrell, J. *Can. J. Phys.* **1969**, *48*, 1242–1253.
(17) Borkman, R. F.; Kearns, D. R. *J. Chem. Phys.* **1966**, *44*, 945–949.
(18) Berendsen, H. J. C.; Postma, J. P. M.; van Gunsteren, W. F.; DiNola, A.; Haak, J. R. *J. Chem. Phys.* **1984**, *81*, 3684.
(19) Weiner, S. J.; Kollman, P. A.; Nguyen, D. T.; Case, D. A. *J. Comput. Chem.* **1986**, *7*(2), 230–252.
(20) (a) Gaussian-82. Binkley, J. S.; Whiteside, R. A.; Raghavachari, K.; Seeger, R.; DeFrees, D. J.; Schlegel, H. B.; Frisch, M. J.; Pople, J. A.; Kahn, L. R. Carnegie-Mellon University, 1982. (b) GAMESS. Dupuis, M.; Spangler, D.; Wendoloski, J. J. National Resource for Computations in Chemistry Software Catalog, University of California: Berkeley, CA 1980, Program QG01. Also see: Schmidt, M. W.; Boatz, J. A.; Baldridge, K. K.; Koseki, S.; Gordon, M. S.; Elbert, S. T.; Lam, B. *QCPE Bulletin* **1987**, *7*(115).
(21) (a) G80-UCSF. Singh, U. C.; Kollman, P. A. *QCPE* **1982**, 446. (b) Singh, U. C.; Kollman, P. A. *J. Comput. Chem.* **1984**, *5*, 129–145.
(22) Pulay, P.; Fogarasi, G.; Pongor, G.; Boggs, J. E.; Vargha, A. *J. Am. Chem. Soc.* **1983**, *105*(24), 7037–7047. Duncan, J. L.; Mallinson, P. D. *Chem. Phys. Lett.* **1973**, *23*(4), 597–599.
(23) Jorgensen, W. L. *J. Phys. Chem.* **1986**, *90*, 1276–1284.
(24) Jorgensen, W. L.; Chandrasekhar, J.; Madura, J. D.; Impey, R. W.; Klein, M. L. *J. Chem. Phys.* **1983**, *79*, 926.
(25) van Gunsteren, W. F.; Berendsen, H. J. C. *Mol. Phys.* **1977**, *34*, 1311–1327.

Table II. Molecular-Mechanical Geometrical Parameters

| geom param[a] | force constant[b] | geom value |
|---|---|---|
| | Acetone | |
| bonds | | |
| C–O | 570.00 | 1.19 |
| C*–O* | 469.00 | 1.35 |
| C–CT | 317.00 | 1.51 |
| C*–CT | 317.00 | 1.51 |
| H–CT | 331.00 | 1.09 |
| H*–CT | 331.00 | 1.09 |
| angles | | |
| H–CT–H | 35.00 | 108.78 |
| H*–CT–H* | 35.00 | 108.18 |
| C–CT–H | 35.00 | 110.15 |
| C*–CT–H* | 35.00 | 110.73 |
| CT–C–O | 80.00 | 121.77 |
| CT–C*–O* | 80.00 | 111.90 |
| CT–C–CT | 70.00 | 116.46 |
| CT–C*–CT | 70.00 | 120.69 |
| specific dihedrals | | |
| O–C–CT–H | 0.82 | 0.00 |
| O*–C*–CT–H* | 1.60 | 180.00 |
| planar constraint | | |
| X–X–C–O | 10.50 | 180.00 |
| | Formaldehyde | |
| bonds | | |
| C–O | 570.00 | 1.18 |
| C*–O* | 469.00 | 1.34 |
| H–C | 340.00 | 1.09 |
| H*–C* | 340.00 | 1.08 |
| angles | | |
| H–C–O | 40.00 | 122.14 |
| H*–C*–O* | 35.00 | 113.32 |
| H–C–H | 35.00 | 115.71 |
| H*–C*–H* | 35.00 | 118.65 |
| planar constraint | | |
| X–X–C–O | 10.50 | 180.00 |
| | Carbon Tetrachloride | |
| bonds | | |
| C–Cl | 222.00 | 1.77 |
| Cl–Cl | 222.00 | 2.89 |

[a] An asterisk designates a $\pi^*$ excited state atom type. CT is acetone's tetrahedral methyl carbon. The force constant for C–Cl is interpolated from the Weiner et al. force field; the Cl–Cl force constant is arbitrarily high to ensure symmetric rigidity, although this was not critical since $CCl_4$ simulations used SHAKE. [b] Force constants are in kcal/mol, bond lengths in Å, angles in deg. The dihedral force constants are actually $V/2$ as input to AMBER.

fied-OPLS methanol did not use SHAKE; rather, a loop-closing "bond" across the methanol hydroxyl hydrogen and united methyl group was used to maintain a rigid $CH_3$–O–H angle. The bond-stretching force constant used was 900 kcal/mol on the loop-closing bond, 320 kcal/mol for the Me–O bond, and 553 kcal/mol for the O–H bond. All other geometric and interaction parameters for methanol were identical with those used by Jorgensen,[24] except in the later simulations involving the acetone $S_0 \rightarrow S_1$ transition in methanol, where the van der Waals parameters used on the united methyl group ($R^* = 4.00$ Å, $\epsilon = 0.190$ kcal/mol) were slightly different than those of Jorgensen. We found that (after extensive MD equilibration of the pure methanol) the use of this modification gave better accord with the experimental volume while retaining the proper internal energy. This makes physical sense in that since this methyl group carries a partially positive charge (+0.265), due to its being immediately adjacent to an electronegative oxygen, one would expect its VDW radii to be somewhat smaller than that of a strictly alkyl methyl group, such as found in ethane. For the pure modified-OPLS methanol, heat of vaporization and density were correct to within a few percent of experiment, and radial distribution functions (not shown) were essentially identical with those reported by Jorgensen. For $CCl_4$, the experimentally determined C–Cl and loop-closing Cl–Cl bond lengths (Table II) were used.[26]

No attempt was made to prefit the interaction parameters so as to specifically reproduce experimental solvent shifts. A simple molecular mechanical potential model was parametrized in a straightforward

(26) Narten, A. H.; Danford, M. D.; Levy, H. A. *J. Chem. Phys.* **1967**, *46*(12), 4875–4880.

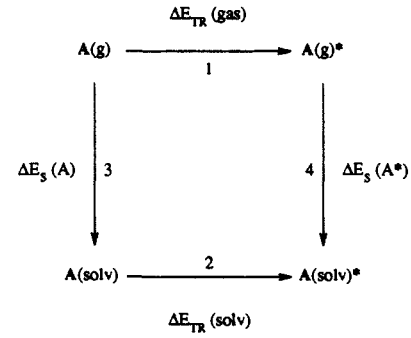


**Figure 1.** Thermodynamic cycle energy perturbation. $\Delta E_s$ is solvation energy. $\Delta E_{tr}$ is electronic transition energy.

"assembly line" fashion, using ab initio calculations and some values already in the literature. This turned out to be adequate to qualitatively reproduce experimentally observed solvent shifts for electronic transitions in several solvents.

### Statistical Mechanical Free Energy Perturbation

The molecular dynamics implementation of the FEP method in the program AMBER[27a,b] was used for the calculation of the difference in Gibbs free energy of solvation for a ground-state solute versus an $n \rightarrow \pi^*$ excited state (the recent AMBER 3.0 Revision A was used in simulations involving $S_1$ acetone). The perturbation is facilitated by changing or "mutating" the values of the parameters of a classical molecular mechanical potential energy function which mediates intermolecular interactions:[28]

$$V_{\text{total}} = \sum_{\text{bonds}} K_r(r - r_{\text{eq}})^2 + \sum_{\text{angles}} K_\theta(\theta - \theta_{\text{eq}})^2 + \sum_{\text{dihedrals}} \frac{V_n}{2}[1 + \cos(n\theta - \gamma)] + \sum_{i<j} \left[ \frac{A_{ij}}{R_{ij}^{12}} - \frac{B_{ij}}{R_{ij}^{6}} + \frac{q_i q_j}{\epsilon R_{ij}} \right]$$

The form and parametrization of this potential function have been discussed in detail.[19] For a list of additional specific parameters used in this study see Tables I and II.

Figure 1 depicts the various paths of the thermodynamic cycle used to calculate the difference in energy for two electronic states of a solute A in a solvent versus gas phase. The differential solvation energies of ground versus solvent equilibrated excited states, $\Delta\Delta G_s$, path 4 minus path 3, could be calculated with FEP theory. But FEP theory requires a "small" perturbation in order to ensure adequate ensemble sampling and to minimize computational artifacts that could be generated by physically unrealistic systems. A solute can be "vanished from" or "grown into" solution in order to calculate absolute solvation energies. However, this approach would require long sampling times and could lead to artifacts. Alternatively, paths 2 and 1 can be directly calculated with the perturbation methodology, so that a "small" perturbation is maintained. The (generic) transition energy $\Delta E_{TR}$(gas) represented by path 1 in the above scheme (Figure 1) is simply equal to the isolated solute excitation energy, and that of path 2 $\Delta E_{TR}$(solv) is the solute excitation energy in solution. The difference between path 2 and path 1, $\Delta E_2 - \Delta E_1$, gives the difference in excitation energy due to the influence of the solvent, which we refer to as either $\Delta\Delta V_s$ or $\Delta\Delta G_s$. When A(solv)* is considered as the Franck–Condon excited state, path 2 minus path 1 is given

(27) (a) Singh, U. C.; Weiner, P. K.; Caldwell, J. W.; Kollman, P. A. AMBER (UCSF), version 3.0, 1986, Department of Pharmaceutical Chemistry, University of California, San Francisco. See also: Weiner, P. K.; Kollman, P. A. *J. Comput. Chem.* **1981**, *2*, 287. (b) Seibel, G.; AMBER 3.0 Revision A, 1990, Department of Pharmaceutical Chemistry, University of California, San Francisco.

(28) In the AMBER potential function $V_{\text{total}}$ is the potential energy of the system; $K_r$ and $r_{eq}$ are the bond stretching constant and equilibrium bond distance; $K_\Omega$ and $\Omega_{eq}$ are the bond angle stretching constant and equilibrium bond angle; $V_n$, $n$, and $\gamma$ are the torsional force constant, periodicity of the torsional term, and the phase angle; $A_{ij}$ and $B_{ij}$ are the (Lennard-Jones) nonbond interaction parameters for particles $i$ and $j$; $R_{ij}$ is the interatomic distance between $i$ and $j$; $q_i$ and $q_j$ are the atomic partial charges on $i$ and $j$; $\epsilon$ is the effective dielectric constant.

by $\Delta\Delta V_s$ and directly corresponds to the UV solvent frequency shift. When A(solv)* is considered as the solvent-equilibrated excited state, path 2 minus path 1 is given by the difference in free energy $\Delta\Delta G_s$ between the ground and solvent-equilibrated excited state.

There could be two contributions to $\Delta\Delta E_{TR}$, one coming from a difference in intrasolute energies, and another coming from solute–solvent interactions. We have assumed that to a good approximation the intrasolute energies (mainly vibrational energies) cancel in the subtraction $\Delta E_2 - \Delta E_1$, and thus a simulation of path 2 gives the change in transition energy due to differential solvation of the solute A, its ground versus excited state.

Theoretical aspects of free energy perturbation methods have been discussed in detail elsewhere,[29] and only the fundamental equations will be recalled here as comments regarding our simulations will relate to these equations. Free energy was calculated via the continuous integration or "slow growth" method as

$$\Delta G = \int_0^1 \left\langle \frac{\delta V(\lambda)}{\delta \lambda} \right\rangle_\lambda d\lambda$$

where $\delta V$ is the difference in potential energies between the reference and the perturbed systems when both are evaluated at the coordinates of the reference system according to the set of states generated by coupling to the parameter $\lambda$ which varies along the integral [0,1] as the trajectory progresses. The free energy via single step (one-window) was also calculated in the usual way

$$\Delta G = -RT \ln \langle \exp(-(V_{perl} - V_{ref})/RT) \rangle_{ref}$$

where the brackets $\langle\ \rangle$ again denote a time average, $R$ is the gas constant, and $T$ is temperature. These two methods should give identical free energy differences in the limit of infinite sampling.

The point charges in the coulombic part of the nonbonded parameters and the parameters for bond lengths and angles were mutated as a function of trajectory time (slow growth) or as a discrete single-interval "flash" perturbation (one-window), using a mutational coupling function of the form

$$P(\lambda) = (\lambda)P_{ref} + (1 - \lambda)P_{perl}$$

where $P_{ref}$ is a parameter assigned to the reference state solute and $P_{perl}$ is the corresponding parameter that is assigned to the perturbed state solute.

When calculating the $\Delta\Delta G_s$ using the "slow growth" method, the FEP theory's assumption of $\Delta G < RT$ for each (micro) window is rigorously met. Using this method, and assuming representative sampling, one may expect to obtain a reliably quantitative $\Delta\Delta G_s$ value, but where the effects of Franck–Condon solute–solvent "strain" (nonoptimal packing and orientation at the instance of transition) are largely lost. These simulations do not correspond directly to an electronic transition, i.e. the transition is artificially "slowed" down, so that solute–solvent equilibration occurs throughout the MD perturbation trajectory, during the transition. These simulations should provide reliable values for the difference in free energy of solvation of the solvent-equilibrated ground state versus solvent-equilibrated excited state.

When sampling over a single perturbation window (one-window method) where the $\Delta G$ involved is greater than several $RT$, FEP theory begins to break down as the fundamental assumption of a "small" perturbation is no longer rigorously met. Some incompleteness of ensemble sampling is probably inevitable in such a situation. In light of this, the calculated $\Delta G$ is usually expected to be less quantitative for one-window perturbations where $\lambda$ jumps directly from $1 \rightarrow 0$ or $0 \rightarrow 1$, e.g. ground-state $\rightarrow$ excited, or excited state $\rightarrow$ ground state all in one step. However, these one-window calculations do facilitate the direct simulation of an electronic transition event in a solvent environment, as $\Delta\Delta V_s$ is also calculated for the ensemble over the MD trajectory. During these simulations the solvent equilibrates about and orients with respect to the reference solute, e.g. the ground state for an absorption. In this example the excited state "flashes" into the solvent cage structure which has been oriented about the ground-state solute, directly modeling what is customarily referred to as the Franck–Condon excited state. Recall that the time required for an electronic transition is of the order of $10^{-15}$ s, while intramolecular relaxation occurs more on the order of $10^{-14}$ to $10^{-13}$ s, and $10^{-13}$ to $10^{-12}$ s for intermolecular reorientations.[30] As a consequence, internuclear distances do not have time to change much during an electronic transition. Only electronic polarization of the solvent responds immediately on excitation. The transition can be considered (prior to nuclear relaxation) to be the superpositioning of the excited-state electronic distribution onto the solute geometry and potential energy surface which was prepared as a result of ground-state solute–solvent interactions. A single window perturbation treatment closely corresponds to this physical situation, although we have omitted solvent electronic polarization. The thermally equilibrated excited state is subsequently reached through relaxation processes, including reorientation of the solvent. A Franck–Condon nonequilibrium state also appears (in the reverse sense) during an emission event. The ensemble configurations generated during the single step, one-window perturbation calculations will be recalled later on as their analysis provides valuable qualitative insight into the influence of solute–solvent and solvent–solvent structuring on the energetics involved in the $n \rightarrow \pi^*$ transition process.

For the one-window runs the $\Delta\Delta V_s$ was calculated (in both forward and reverse directions) at every MD step and averaged over the entire trajectory, facilitating the calculation of the difference in solvation free energies of the ground- and excited-state solutes. Several individual calculations were performed for each perturbation, each from different pre-equilibrated starting configurations, and the values of each of the separate calculations were averaged (time-weighted) to give the overall $\Delta\Delta V_s$ and $\Delta\Delta G_s$.

The usual procedure when using windows is to equilibrate about and perturb with respect to one reference state and then to do the same for the opposite state, taking the average of these two calculations as the $\Delta G$ value for that window. One expects this to give a more quantitative value for one-window calculations. In particular, such double-wide sampling ordinarily leads to a more thorough representation of the surface and hopefully at least a partial cancelling of hysteresis effects. It is the averaged $\Delta\Delta G_s$ of the forward and reverse single-step simulations that should be considered as the value corresponding to the difference in free energy between the solvent-equilibrated ground state and the solvent-equilibrated excited state. In short, for our two roughly similar systems, i.e. a single ground- or excited-state solute in a periodic box of solvent, the generation of samples using either electronic state as the reference essentially provides a complementary ensemble that enhances information about the difference in energy between different areas of the potential surfaces.[31] One may also note (Table III) the general agreement between the one-window (forward and reverse averaged) calculations with the

(29) (a) van Gunsteren, W. F. *Methods for Calculation of Free Energies and Binding Constants; Successes and Problems*; Weiner, P., Ed.; Proceedings of the Free Energy Perturbation Colloquium, Princeton, Dec. 1987. (b) Pearlman, D. A.; Kollman, P. A. In *Computer Simulation of Biomolecular Systems: Theoretical and Experimental Applications*; van Gunsteren, W. F.; Weiner, P. K., Eds.; Escom Science Publishers: Netherlands, 1989; pp 101–119. (c) Singh, U. C.; Brown, F. K.; Bash, P. A.; Kollman, P. A. *J. Am. Chem. Soc.* **1987**, *109*(6), 1607–1614.

(30) (a) Ohmine, I. *J. Chem. Phys.* **1986**, *85*, 3342. (b) Levy, R. M.; Kitchen, D. B.; Blair, J. T.; Krogh-Jespersen, K. *J. Phys. Chem.* Submitted. In particular, Levy et al. have found that in the solvent (water) equilibration of $S_1$ excited-state formaldehyde, the major part of the relaxation requires only about 200 fs.

(31) Due to the incompleteness of sampling over the reference and perturbed potential surfaces (because $\Delta\Delta G$ is large for one window) and the biasing of free energy differences due to the one-window FEP equation's treatment of the Franck–Condon surfaces as if they were populated in a boltzman distribution, the one-window free energy values are not reliable when considered in only one perturbation direction, i.e. they must be averaged. The one-direction values should not therefore be used as evidence for any solvent-mediated shifting of the $n \rightarrow \pi^*$ 0–0 band in an emission versus an absorbance, nor are they interpretable as the difference in free energy of solvation between a thermally equilibrated state and a Franck–Condon state.

**Table III.** Free Energy Perturbation Results

| transition[a] | solvent | $time_{SG}$[b] | $\langle\Delta\Delta G_{SG}\rangle$[c] | $time_{1W}$ | $\langle\Delta\Delta G_{1W}\rangle$ | $\langle\Delta\Delta V_{1W}\rangle$[d] | expt[e] |
|---|---|---|---|---|---|---|---|
| $A \rightarrow A^*(T_1)$ | H2O | 42 | 4.52 | 100 | 4.0 ± 1.5 | 6.2 ± 1.7 | |
| $A^*(T_1) \rightarrow A$ | H2O | 92 | −4.64 | 138 | −6.0 ± 1.8 | −2.8 ± 1.9 | |
| $A \rightarrow A^*(S_1)$ | H2O | 50 | 3.86 | 150 | 3.3 ± 1.1 | 4.8 ± 1.4 | 4.46 (5.78) |
| $A(^*S_1) \rightarrow A$ | H2O | 100 | −3.80 | 100 | −4.8 ± 1.4 | −2.5 ± 1.7 | |
| $average_{S0\rightarrow S1}$ | | | 3.83 | | 4.0 ± 1.3 | | |
| $A \rightarrow A^*(T_1)$ | MEOH | 50 | 2.32 | 87 | 2.7 ± 0.9 | 5.0 ± 1.8 | |
| $A^*(T_1) \rightarrow A$ | MEOH | 50 | −3.34 | 60 | −2.3 ± 0.9 | −1.3 ± 1.1 | |
| $A \rightarrow A^*(S_1)$ | MEOH | | | 250 | 1.9 ± 0.9 | 4.0 ± 1.9 | 2.40 (4.18) |
| $A^*(S_1) \rightarrow A$ | MEOH | | | 200 | −3.7 ± 1.9 | −1.2 ± 1.2 | |
| $average_{S0\rightarrow T1,S1}$ | | | 2.83 | | 2.7 ± 1.3 | | |
| $A \rightarrow A^*(T_1)$ | $CCl_4$/STO-3G[f] | | | 39 | 0.0 ± 0.2 | 0.0 ± 0.1 | |
| $A \rightarrow A^*(T_1)$ | $CCl_4$/6-31G*[f] | | | 56 | 0.2 ± 0.2 | 0.3 ± 0.3 | −1.43 (0.00) |
| $A^*(T_1) \rightarrow A$ | $CCl_4$/6-31G*[f] | | | 30 | −0.2 ± 0.3 | −0.1 ± 0.2 | |
| $A \rightarrow A^*(T_1)$ | $CCl_4/\Omega$=15DA² | | | 22 | 0.6 ± 0.4 | 0.8 ± 0.6 | |
| $A^*(T_1) \rightarrow A$ | $CCl_4/\Omega$=15DA² | | | 16 | −0.5 ± 0.4 | −0.2 ± 0.6 | |
| $average_{S0\rightarrow T1}$ | /6-31G* | | | | 0.2 ± 0.2 | | |
| $F \rightarrow F^*(T_1)$ | H2O | 71 | 2.93 | 166 | 2.7 ± 1.0 | 4.4 ± 1.3 | |
| $F^*(T_1) \rightarrow F$ | H2O | 50 | −3.20 | 111 | −3.6 ± 1.4 | −1.8 ± 0.6 | |
| $average_{S0\rightarrow T1}$ | | | 3.04 | | 3.2 ± 1.2 | | |
| $F \rightarrow F^*(T_1)$ | $CCl_4$/STO-3G[f] | 28 | 0.04 | 37 | 0.1 ± 1.0 | 0.1 ± 0.2 | |
| $F^*(T_1) \rightarrow F$ | $CCl_4$/STO-3G[f] | 14 | 0.08 | | | | |
| $average_{S0\rightarrow T1}$ | | | 0.05 | | 0.1 ± 0.1 | | |

[a] A indicates acetone ground state, A* the excited state, and similarly F and F* for formaldehyde. [b] $TIME_{SG}$ and $TIME_{1W}$ are total times in picoseconds for slow growth and one-window molecular dynamics. [c] The absolute magnitudes of the forward and reverse $\Delta\Delta G$ values were averaged and are reported as positive. Slow growth $\Delta\Delta G_{SG}$ were averaged with use of time weighting since they are essentially equivalent ensembles. One-window runs $\Delta\Delta G_{1W}$ were simple averaged since they represent nonidentical ensembles and are reported with the standard deviations of their values as collected over the FEP-MD trajectories. [d] $\Delta\Delta V_{1W}$ are differences in potential energy of solvation for ground versus excited states. [e] EXPT is the spectroscopically measured frequency shift converted to energy (kcal/mol). Experimental blue shifts (without parentheses) were determined at $\lambda_{max}$ for absorption, by Bayliss and McRae[10] for water and $CCl_4$, see ref 4 for methanol. Shift values in parentheses are from: Suzuki, H. *Electronic Absorption Spectra and Geometry of Organic Molecules*; Academic Press: New York, 1967; p 99. [f] Basis sets from which $CCl_4$ charges were derived, $\Omega$=15DA² indicates charge model when octapole moment is fitted.

more rigorous slow growth method.

### Free Energy and Potential Energy Results

The calculated average $\Delta\Delta V_s$ and $\Delta\Delta G_s$ values are compared to spectroscopically measured solvent dependent frequency shift values that were available (see Table III). The calculated values exhibit the proper trend, i.e. the $n \rightarrow \pi^*$ transitions shift further toward the blue as successively more polar solvents are considered. The experimental shift values in terms of kcal/mol for acetone solute in water, in methanol, and in $CCl_4$ are listed in Table III (column 8) as 4.46, 2.40, and −1.43 respectively, along with an alternative set of values (5.78, 4.18, 0.00) from a second source (which may be slightly less rigorous) listed in parentheses. The forward (e.g. $A \rightarrow A^*$) one-window $\Delta\Delta V_{1W}$ values are comparably close to those of experiment, and quantitative within a single standard deviation (1 SD) for water and methanol solvents when the $S_0 \rightarrow S_1$ transition is considered. The average $\Delta\Delta V_{1W}$'s calculated (column 7) are 4.75 ± 1.38 and 3.96 ± 1.89 for acetone's $S_0 \rightarrow S_1$ transition in water or in methanol, respectively. For $CCl_4$, $\Delta\Delta V_{1W}$ is 0.25 ± 0.28 with use of the 6-31G* charge model. Regardless of the $CCl_4$ charge model used, $\Delta\Delta V_{1W}$ values were always slightly positive, with oscillations occasionally carrying over into negative shift energies for acetone's $S_0 \rightarrow T_1$ transition.

Using data tabulated in Table III, one can graphically illustrate (Figure 2) the effects of solvent on the shifts of absorption or emission frequency. The arrow-headed "transition" lines are not drawn to full scale since the absolute magnitude of the $n \rightarrow \pi^*$ transition is near 102.1 kcal/mol (2800 $cm^{-1}$), and the solvent effects are on the order of kilocalories, thus the broken transition lines. However, the calculated state-to-state endpoint levels (represented by the horizontal lines), the calculated (1 SD) standard deviations (represented by rotated parentheses), and the experimental data points (represented by asterisks) are all correctly positioned relative to one another on this scale. All of the calculated $\Delta\Delta V_{1W}$ results are in reasonable agreement with experiment. The calculated values are within the range of the dual sets of experimental values for water and methanol, but they blue shift slightly too far in the $CCl_4$ case. Note that the calculations never give a shift that is too far toward the red when compared to their corresponding experimental values. Also note that the experimental data points are within the reported calculated standard deviations for water and methanol.

One can see at a glance (as per Haberfield's earlier experimental findings) that the $n \rightarrow \pi^*$ blue shift that occurs on transferring acetone from $CCl_4$ to a dipolar, hydrogen-bonding solvent is due not only to superior solvation of the ground state but also to the inferior solvation of the excited state in these dipole hydrogen bond donor solvents (Figure 2). This is especially true in the case of methanol (keep in mind that the true shift in $CCl_4$ is even further to the red than our calculated value).

The calculation of $\Delta\Delta G_s$, represented by the dashed arrow-headed lines, has facilitated the determination of the solvent-equilibrated excited-state solvation energy and its positioning within this scheme. Knowing this also permits the determination of the Franck–Condon radiative emission state solvation energy. The interesting structural changes that occur on solvent equilibration of the Franck–Condon states will be examined in detail later in this paper.

The corresponding (forward/reverse averaged) $\Delta\Delta G_{1W}$ values (Table III, column 6) are 4.03 ± 1.27, 2.70 ± 1.32, and 0.22 ± 0.23 in water, methanol, and $CCl_4$, respectively, where again the (1 SD) standard deviations indicate the partial range of free energy values encountered over the ensemble. The $\Delta\Delta G_s$ between the ground *equilibrated* and excited *equilibrated* states (the value obtained from FEP calculations) should always be less blue shifted compared to the $\Delta\Delta V_s$ between the ground *equilibrated* state and the *Franck–Condon* excited state (the value analogous to spectroscopic data). This must be the case since on equilibration from the Franck–Condon excited (solvent-strained) state, the overall system free energy optimizes, lowering the excited-state solvation free energy. This behavior is reproduced in all of our calculations, i.e. $\Delta\Delta G_s < \Delta\Delta V_s$.

There are several possible reasons why the FEP calculations (particularly in the methanol and $CCl_4$ cases) give an average $\Delta\Delta G_s$ that corresponds to a frequency shift slightly further into the blue than the experimental shift. One reason is the neglect

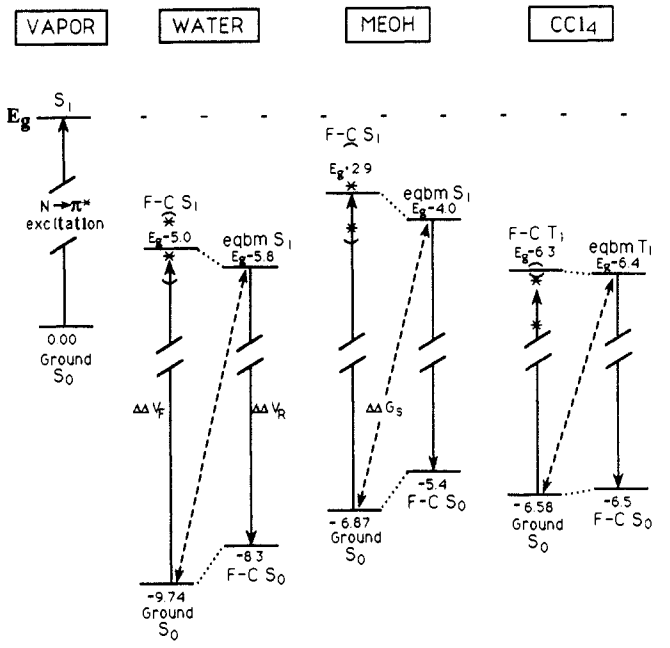


**Figure 2.** Differential solvation of acetone's ground vs n → π* excited state in three solvents. All values listed in the figure can be arrived at from data in Table III. $E_g$ is the excitation energy in the gas phase. The $S_0$ ground state is taken as the 0.0 energy level. Energies lower than 0.0 are due to solvation of ground states; energies lower than $E_g$ (but above 0.0) are due to solvation of excited states. The states are referred to as ground, F-C (Franck-Condon), or eqbm (solvent equilibrated). The symbols $\Delta\Delta V_F$ and $\Delta\Delta V_R$ refer to the forward and reverse (absorption and emission) shift energies and are placed beside the transition line for which the shift is calculated. The lowermost asterisks designate the (presumably) best spectroscopic data; upper asterisks designate alternative spectroscopic data. Rotated parentheses indicate ±1 standard deviation from calculated values. Also see text.

of explicit electronic polarizability in the potential function and the related fact that the solvent models were designed to have enhanced permanent polarities in an attempt to cause their effective two-body pair potentials to account (in an average way) for this neglect of explicit polarizability. Also, differences in the dispersion interactions between solute and solvent for ground versus excited states were not explicitly modeled. The unavoidable incompleteness in sampling is always an issue, and our comparison of n → π* (0–0) calculated difference-energy values with spectroscopic blue shift values reported for n → π* ($\lambda_{max}$) may have some bearing on the agreement between theory and experiment.

There is a physically relevant reason involving the relative differences between the ground- and excited-state solute dipole moments when considering the $S_1$ versus $T_1$ excited states. For formaldehyde, $\Delta\mu_{(GS\text{-}S1)expt}$ = 0.77 D, $\Delta\mu_{(GS\text{-}T1)expt}$ = 1.04 D, and $\Delta\mu_{(GS\text{-}T1)calc}$ = 1.11 D as per experimental measurements or ab initio wave functions used here for formaldehyde (see Table I and Methods section). Although no experimental measurement of the excited-state dipole moment was found for acetone, we would also expect that $\Delta\mu_{GS\text{-}T1}$(acetone) > $\Delta\mu_{GS\text{-}S1}$(acetone). The ab initio calculations do give this trend for the acetone states: $\Delta\mu_{(GS\text{-}S1)calc}$ = 1.26 D and $\Delta\mu_{(GS\text{-}T1)calc}$ = 1.36 D. On the basis of the above listed $\Delta\mu$'s, an $S_0 \rightarrow T_1$ absorption should then be expected to produce an n → π* band which shifts slightly further toward the blue when compared with absorption to an $S_1$ state. Our calculations reflect this difference of $T_1$ versus $S_1$ dipole moment magnitudes in the larger difference energies calculated for the $S_0 \rightarrow T_1$ transition, which comes about as a result of the less favorable solvation of the less (di-)polar $T_1$ state. Although solvent shift data for carbonyl n → π* transitions directly to the triplet are not available, the ordinarily spin-"forbidden" $S_0 \rightarrow T_1$ absorption does occur as a weak magnetic dipole transition (via spin–orbit coupling) for formaldehyde and carbonyl compounds in general.[13a,b] Recall that the spectroscopically measured values (solvent shifts) which we use for comparisons correspond to the $S_0 \rightarrow S_1$ transition. The $\Delta\Delta G_s$ (forward/reverse, averaged) calculated for the $S_0 \rightarrow T_1$ in methanol (2.43 kcal/mol) is apparently slightly out of order with this trend, a result that may be due to insufficient sampling, and/or use of the different united-methyl VDW parameters as described in the Methods section.

No reliable spectroscopic shift value was found for formaldehyde, which is 99.95% diol in aqueous media. Acetone remains 99.8% ketone, i.e. less than 0.2% diol and less than 0.0001% enol in aqueous media (25 °C).[32] On the basis of the absolute magnitudes of their experimentally measured dipole moments (see Table I), and the $\Delta\mu_{GS\text{-}XS}$ given by the calculated dipole moments, one naturally expects a smaller effect in the differential solvation of ground versus excited states for formaldehyde as compared to acetone. It follows that $\Delta\Delta E_{tr}$ should be of smaller absolute value for formaldehyde than for acetone, and this is predicted by the calculations, i.e. for the $S_0 \rightarrow T_1$ transition in water (Table III): $\Delta\Delta V_s$(formaldehyde) ≈ 4.4, $\Delta\Delta V_s$(acetone) ≈ 6.2 kcal/mol, and $\Delta\Delta G_s$(formaldehyde) ≈ 3.0 kcal/mol while $\Delta\Delta G_s$(acetone) ≈ 4.6 kcal/mol (free energies as per the "slow growth" calculations). Blair et al. argue on the basis of related available data that the true solvent shift exhibited by monomeric formaldehyde in water is likely to be in the 600–1900 $cm^{-1}$ range. Our calculated value of $\Delta\Delta V_s$, 4.4 kcal/mol (1530 $cm^{-1}$), is consistent with their estimate.[34a]

The absence of polarizability terms in the molecular mechanical potential, along with the omission of explicit modeling of the differences in the solute–solvent van der Waals interactions for ground versus excited states, accounts for the inability of the simulation to reproduce the red shift of n → π* carbonyl transitions in $CCl_4$. As mentioned in the introduction, *all* solvents electronically polarize (to varying degrees), facilitating the formation of an electronic transition moment in a solute, and thus contribute toward an n → π* red shift relative to the vapor-phase transition. Also, since the electronically more diffuse excited-state solutes are "larger" and more polarizable, attractive solute–solvent dispersion interactions may be stronger even in the nonequilibrium Franck–Condon excited state, again contributing to a red shift relative to the vapor phase. Since $CCl_4$ is a nonorienting, nonpolar solvent, these contributions to a red shift due to the interaction of the solute with the large polarizable chlorine atoms are the major solvent influences on carbonyl n → π* transitions in $CCl_4$.

Several $CCl_4$ models were examined in this study (see Table I). The STO-3G basis set gives a $CCl_4$ with slightly negative chlorines and a positive carbon, whereas the 6-31G* basis set gives charges of the opposite sign and slightly greater magnitude. The van der Waals parameters used were those of McDonald et al.[33] with slight modifications to the chlorine parameters to ensure proper fit to the heat of vaporization and density for pure $CCl_4$ (we adopted the formula Jorgensen uses[24] for determination of $\Delta H_{vap}$). These simulations resulted in energy values that oscillated near 0.0 kcal/mol (Table III). A third $CCl_4$ model used the permanent point charges (+0.30 Cl, −1.20 C) that McDonald et al. have suggested should reproduce a reasonable octapole moment, estimated as Ω = 15 D Å$^2$, for $CCl_4$.[33] The strong permanent (non-induced) field created by these charges caused the FEP calculations to reproduce even less adequately the red-shift character of the carbonyl n → π* transition in $CCl_4$ (Table III). A simulation using these same charges but with reversed signs gave approximately the same results. Thus, using a simple (no explicit polarization) two-body potential we found that charge–charge interactions could not account for the experimentally observed red shift. The red shift of the carbonyl n → π* band

(32) (a) Bell, R. P. *Adv. Phys. Org. Chem.* **1966**, 4, 1 (diol percentages for F and A). (b) Bell, R. P.; Smith, P. W. *J. Chem. Soc. B* **1966**, 241.

(33) McDonald, I. R.; Bounds, D. G.; Klein, M. L. *Mol. Phys.* **1982**, *45*(3), 521–542.

(34) (a) Blair, J. T.; Krogh-Jespersen, K.; Levy, R. M. *J. Am. Chem. Soc.* **1989**, *111*, 6948–6956. (b) Herman, M.; Berne, B. *J. Chem. Phys.* **1983**, *78*, 4103. (c) Warshel, A.; Levitt, M. *J. Mol. Biol.* **1976**, *103*, 227. (d) Warshel, A.; Russell, S. T. *Q. Rev. Biophys.* **1984**, *17*, 283. (e) Cieplak, P.; Bash, P.; Singh, U. C.; Kollman, P. A. *J. Am. Chem. Soc.* **1987**, *109*, 6283. (f) Madura, J. D.; Jorgensen, W. L. *J. Am. Chem. Soc.* **1986**, *108*, 2517. (g) Bash, P. A.; Field, M. J.; Karplus, M. *J. Am. Chem. Soc.* **1987**, *109*, 8092.

**Table IV.** Potential Energies of Interaction

| system[a] | INTN BETW[b] | NUM CRDS[c] | NUM RES[d] | NUM HBOND[e] | HBOND ENERGY[f] | ELECTR ENERGY[g] | VDW ENERGY | MONO/BULK ENERGY |
|---|---|---|---|---|---|---|---|---|
| A/H2O | u-n | 1600 | 135 | 1.90 | -3.94 | -12.02 | -7.56 | -19.58 |
| A*-FC/W | u-n | 1600 | 135 | 0.50 | -2.72 | -5.79 | -7.56 | -13.35 |
| A*/H2O | u-n | 1195 | 135 | 0.18 | -2.79 | -3.02 | -7.72 | -10.74 |
| A-FCE/W | u-n | 3195 | 135 | 1.39 | -3.67 | -5.82 | -7.68 | -13.50 |
| A/H2O | n-n | 2795 | 96 | 3.32 | -4.40 | -23.25 | 3.06 | -20.19 |
| A/MEOH | u-n | 3300 | 79 | 1.13 | -5.50 | -10.13 | -6.95 | -17.08 |
| A*-FC/M | u-n | 3300 | 79 | 0.53 | -3.04 | -4.87 | -6.95 | -11.82 |
| A*/MEOH | u-n | 3000 | 80 | 0.01 | -2.90 | -1.71 | -7.92 | -9.63 |
| A-FCE/M | u-n | 3000 | 80 | 0.18 | -3.02 | -2.91 | -7.92 | -10.83 |
| A/MEOH | n-n | 6300 | 61 | 1.96 | -5.73 | -16.33 | -1.52 | -17.82 |
| A/$CCl_4$ | u-n | 920 | 61 | 0.00 | | -0.47 | -10.64 | -11.11 |
| F/H2O | u-n | 550 | 122 | 1.54 | -2.98 | -8.16 | -4.30 | -12.46 |
| F*/H2O | u-n | 418 | 133 | 0.02 | -2.35 | -2.35 | -3.81 | -6.16 |
| F/$CCl_4$ | u-n | 12 | 107 | 0.00 | | 0.16 | -6.36 | -6.21 |

[a] All of these values are the result of analysis of configurations saved from the ensembles generated during the calculation of free energy values in Table I. For the system A*-FC/W, acetone's excited $T_1$ state molecular mechanical parameters are superposed onto the ground-state geometry in an ensemble generated by equilibrating a ground-state acetone in water; this is the Franck–Condon (F–C) excited state. A-FCE/W is the F–C emission state for acetone in water. Similarly for A*-FC/M and A-FCE/M in methanol. All other systems are thermally equilibrated solutes. The $CCl_4$ charges were derived from the 6-31G* basis set for A/$CCl_4$, from STO-3G/esp for F/$CCl_4$. [b] INTN BETW indicates whether the interaction examined is between solute–solvent (u–n), or solvent–solvent (n–n). The n–n data are the average of values of the two ensembles, with either A or A* present. [c] The number of saved coordinate sets over which the table quantities were averaged. The time increment between collection of ensemble configurations varied from every 20 to 50 steps or approximately every 0.05 to 0.10 ps. [d] NUM RES is the average number of solvent residues per configuration that are within the nonbond cutoff sphere and thus directly interacting with the monomer of interest. [e] NUM HBOND is the average number of hydrogen bonds formed between a monomer and the solvent (having dimer pair interaction energy ≤-2.5 kcal/mol). [f] HBOND ENERGY is the average energy of H bonds. [g] ELECTR ENERGY is the electrostatic component, and VDW ENERGY is the van der Waals component, which sum to give MONO/BULK ENERGY, the average potential energy of interaction between a monomer and the bulk solvent.

in $CCl_4$ appears to be an induction and/or dispersion effect. These results indirectly indicate theoretical support for Bayliss's elucidation[10a] of a plausible mechanism for the polarization red shift, although we feel that the effect of differential dispersion interactions between the ground- and excited-state solutes and the solvent (which Bayliss ignores) may also figure prominently in the production of the n → π* red shift in nonpolar solvents.

Note that induced-field polarization effects are also neglected in the simulations involving the polar solvents. In reality, these effects are operating but are far overshadowed by the presence of stronger dipole–dipole interactions. Also, since water and methanol are much less polarizable than $CCl_4$, this red-shift contribution is expected to be smaller in these solvents. If the shift toward the red contributed by a (Bayliss type) polarization response were "added in" as a correction to the results from the calculations presented here, all of the values would shift in the correct direction, toward closer agreement with the (presumedly) more rigorous spectroscopic data. The molecular electronic polarizabilities of the three solvents used in this study go as $CCl_4$ > methanol > water. In this regard, it is interesting to note that our $\Delta\Delta V_s$ values (taking the acetone $S_0 \rightarrow S_1$ values for water and methanol and either the 6-31G* or octapole reproducing $CCl_4$ model) are furthest from the experimental values for the solvent ordering $CCl_4$ > methanol > water. Notice (in Figure 2) that across the progression from water to $CCl_4$ the calculated shift values proceed toward the "blue" end of the range of experimental values and that the experimental values "drift" out of the range of the standard deviations in this same order. Thus it appears that where our calculations are not in strict agreement with experiment, they are "off" in the sense that they *should* be, in light of our having neglected explicit electronic polarizability and quantum effects.

### Desolvation of Solute on Solvent Reorientation

During solvent rearrangement about the excited state prior to emission, further alteration of the solute's energy occurs. On release of Franck–Condon orientation strain, the overall system solvation free energy decreases. Commonly, it is assumed that when solvent relaxation occurs around an excited molecule, this brings about more favorable solvation of that particular molecule. However, for systems in which the solute–solvent interaction is mediated primarily by dipole–dipole (orientational) electrostatics, and where the solute is more strongly polar in the ground state than in the excited state, consider the following data:

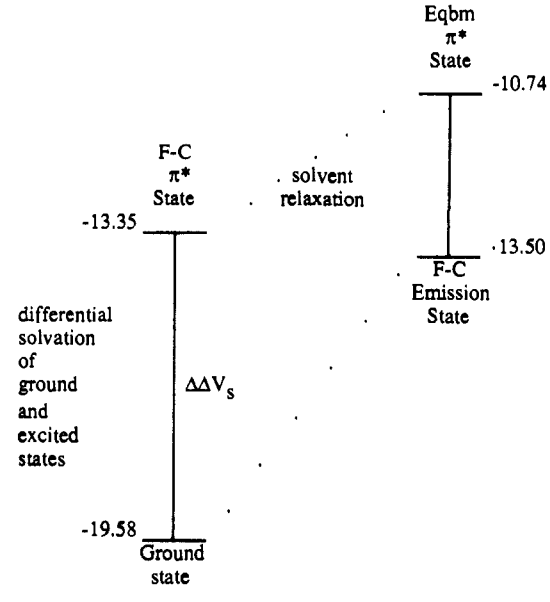


**Figure 3.** Solute–solvent interaction energies $\Delta\Delta V_s$ for acetone $S_0 \rightarrow T_1$ in TIP3P water.

A diagram of the solute's relative energy levels can be constructed from the absolute potential energies of solvation for the ground, Franck–Condon, and excited-state solutes (⟨monomer-bulk energy⟩ presented in Table IV). The diagram presented for acetone in water (Figure 3) illustrates quantitatively that, at least in enthalpic terms, desolvation of the Franck–Condon excited-state solute occurs during thermal equilibration after absorbance. Also, at the first instance upon emission, a Franck–Condon ground state occurs in which the monomer solvation energy is higher (less favorable) relative to the solvent rearranged state, which occurs within picoseconds later. The energy levels in this diagram represent the solute–solvent interaction potential energies during the various stages of an absorption/emission event and not the levels of overall system energy.

For acetone (and formaldehyde which is not shown, but see ref 34a) the radial distribution functions $g$(O–H) for the carbonyl

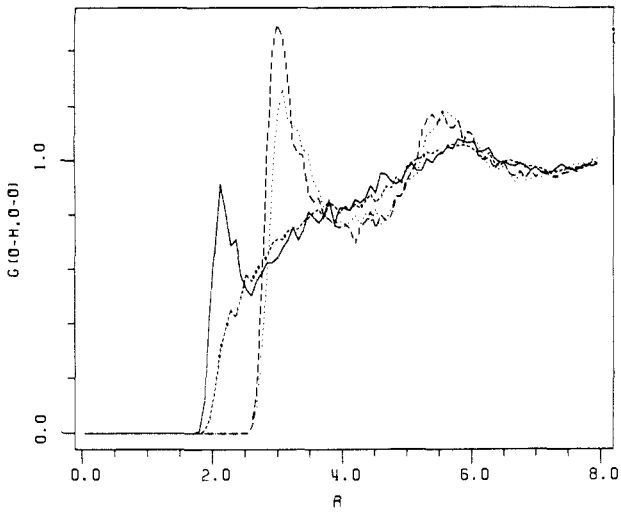


Figure 4. Acetone–water site–site radial distribution functions. Ground state: $g$(O–H), solid line; $g$(O–O), long dashes. $\pi^*(T_1)$ excited state: $g$(O–H), short dashes; $g$(O–O), dots. $R$ is the distance in angstroms.

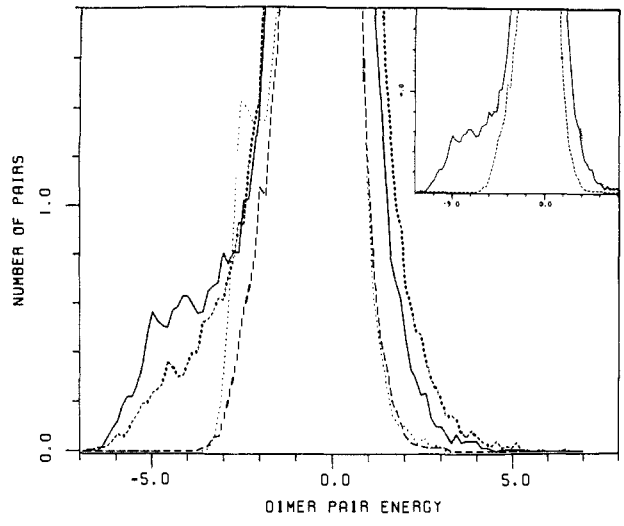


Figure 5. Acetone–water dimer energy distribution functions: equilibrated ground state, solid line; Franck-Condon $T_1$ excited state, dots; equilibrated $T_1$ excited state, longest dashes; Franck-Condon emission state, short dashes. Inset: water–water distribution function, light line; others are the same as above.

oxygen and water hydrogen (Figure 4) illustrate that on average the hydrogen of water, which is in position to hydrogen bond with the carbonyl oxygen, rotates back toward the bulk solvent during thermal equilibration of the excited state. Note (Figure 4) the well-defined hydrogen bond that forms between the ground-state solute and water. Acetone's carbonyl oxygen to first shell water oxygen distance is about 3.0 Å on average (origin to highest first shell oxygen peak, longest dashed line) and about 3.1 Å for formaldehyde (not shown), typical for hydrogen bonds. Note that since the first shell water hydrogens are located at about 2.1 Å (solid line) and since the equilibrium O–H bond length for TIP3P waters is 0.96 Å, the O···H—O angle must be near 180° on average, marking the presence of linearly oriented hydrogen bonds between the solute and solvent. This ground state average solute–solvent orientation, optimally oriented for hydrogen bonding and dipolar interactions, applies equivalently to the Franck–Condon excited state. But after solvent reorientation about the excited state, the near-shell hydrogen peak is substantially reduced (Figure 4, short dashes); only a hydrogen bond remnant remains. The number of hydrogen bonds (defined as less than or equal to −2.5 kcal/mol dimer pair potential energy) for each solute state is quantitated in Table IV. In our simulations, acetone formed 1.9 hydrogen bonds to water on average, and these are (mostly) lost on excitation, leaving 0.50 of a hydrogen bond in the Franck–Condon state, and only 0.18 of a hydrogen bond remaining after thermal equilibration of the excited state. Even though the near-shell solvents reorient to take best advantage of interactions with other (bulk) solvents, a near-shell water's "second" hydrogen still faces toward the excited-state carbonyl oxygen a certain fraction of the time.

The strong ground-state dipole (as opposed to the weaker excited-state dipole) empowers the ground-state solute with a greater ability to command the near-shell solvent configuration on the basis of strong solute–solvent interactions. On solvation of the ground state, the solvent sacrifices some attractive solvent–solvent interactions in order to accommodate the dipolar, hydrogen bonding solute. The solute–solvent interaction energy lowers overall system energy, while the average solvent–solvent interaction energy becomes somewhat higher. The solvent becomes orientationally saturated for solute–solvent dipolar and hydrogen bonding interactions during equilibration of the ground state.

On absorption to the Franck–Condon state, the excited solute thus enjoys a solvent configuration that is optimally oriented so that it can take full advantage of any weak hydrogen bonding or dipolar interactions involving its reduced dipole. Then during equilibration in the presence of the now weakly dipolar, relatively non-hydrogen bonding excited-state solute, the system free energy minimizes when the solvent reorients to regain dipolar and hydrogen-bonding interactions with other solvent molecules, those interactions that were traded away when the ground-state solute was originally solvated. The solvent relaxation proceeds in order to minimize the overall system free energy, not to accommodate the excited-state solute. If the acetone excited state were to then undergo a radiative transition back to the ground state, approximately 1.35 (Table IV) hydrogen bonds could form in the Franck–Condon emission state that occurs prior to equilibration of the renewed ground state.

The monomer-to-bulk energy distribution function for water (Figure 5) graphically displays this loss of solute monomer to bulk solvent interaction energy on excited-state equilibration. A plot for water–water monomer to bulk energy distribution is also shown in the inset (light line) for comparative purposes. This curve was generated with one solute present but should essentially reflect the pure water energy distribution function. These curves are interpreted as the number of solute–solvent dimers ($y$-axis) with a particular interaction energy ($x$-axis) that the solute of interest forms on average. These are solvent–solvent dimers in the case of the pure solvent. The large peaks centered around zero energy are due to the many long-range interactions. The area under the peak in the negative energy region (solid line) reflects hydrogen-bonding interactions between the ground-state solute and equilibrated waters. Note that due to optimal solvent orientation in the Franck–Condon excited state (dots), electrostatic interactions are enhanced in the area of −2 to −3 kcal/mol. The thermally equilibrated $\pi^*$ excited-state solute (longest dashes) curve indicates the loss of strong hydrogen bonds. Only minimal hydrogen bonding or dipolar interactions remain in the area of −2 to −3 kcal (see also Table IV for quantitation). Finally, in the Franck–Condon emission state (short dashes) some hydrogen bonding is immediately recovered, even in a solvent that has equilibrated about the excited-state solute. Illustrated in these plots is a progressive loss of hydrogen bonds and dipolar interactions during the transition process from ground state to Franck–Condon state to equilibrated excited state, and the progressive recovery of these interactions upon emission and reequilibration about the ground state.

In methanol, as in water, the excited-state solute molecule is desolvated relative to the ground-state solute (Figure 6). Again, there is strongly oriented hydrogen bonding between ground-state acetone and the near-shell methanol (see Figure 7). The acetone–methanol oxygen-to-oxygen distance is 2.7 Å, with the methanol hydrogen at 1.75 Å, giving a closer hydrogen bond than in TIP3P water. Since the equilibrium O–H bond length for modified-OPLS methanol is 0.95 Å, the O···H—O angle is again linear on average. Solute–solvent hydrogen bonds, numbering 1.13 in the ground state, are diminished to 0.53 in the Franck-

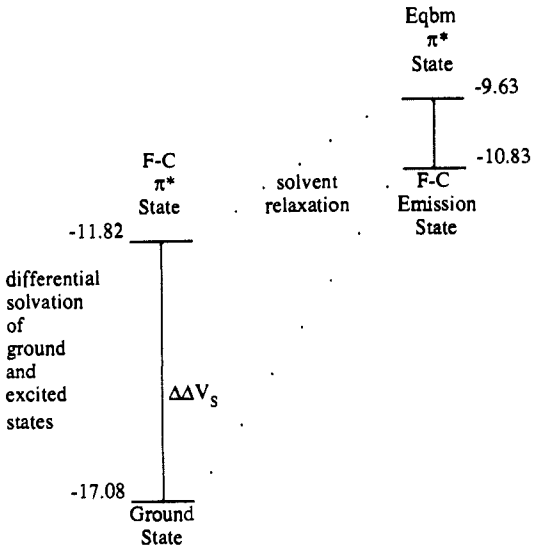


**Figure 6.** Solute–solvent interaction energies $\Delta\Delta V_s$ for acetone $S_0 \rightarrow T_1$ in modified-OPLS methanol.

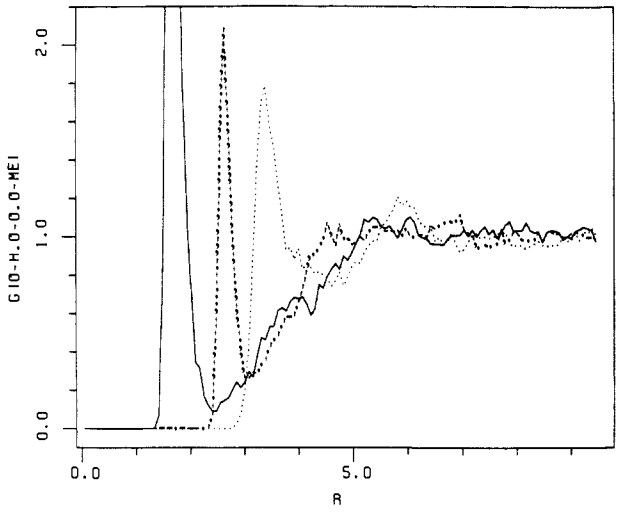


**Figure 7.** Ground-state acetone–methanol site–site radial distribution functions: $g$(O–H), solid line; $g$(O–O), dashes; $g$(O–Me), dots. $R$ is in angstroms.

Condon excited state, and totally lost on equilibration, as indicated in the Table IV.

The radial distribution functions for acetone in methanol $g$(O–H), $g$(O–O), $g$(O–Me) for ground (Figure 7) versus excited state (Figure 8) illustrate that the hydroxyl group of methanol has made an about-face away from solute–solvent hydrogen-bonding configuration during excited-state equilibration. Although coordination number plots have been omitted for clarity, their calculation confirmed that (as indicated in the rdfs) methanol's first shell atoms line up nearest the carbonyl oxygen in the order H, O, Me for the ground state and as Me, O, H in the excited state. This precludes the possibility of the excited state forming even an opportunistic hydrogen bond remnant as occurs in water.

The monomer-to-bulk energy distribution function for acetone in methanol (Figure 9) displays the pair energies for ground-state acetone–methanol (solid), Franck-Condon excited acetone–methanol (dots), equilibrated excited-state acetone–methanol (longest dashes), and Franck-Condon emission state (short dashes), along with the pure methanol–methanol (light line in inset) distribution function for comparison. Note that there is formation of some strong hydrogen bonds between ground-state acetone and the methanol solvent (peak at about −7 kcal/mol, solid line), as well as some general electrostatic interactions (beginning at about −3 kcal/mol) that are more favorable than those for methanol–methanol (light line in inset). There is a progressive diminishing of these general electrostatic interactions as the monomer dipoles

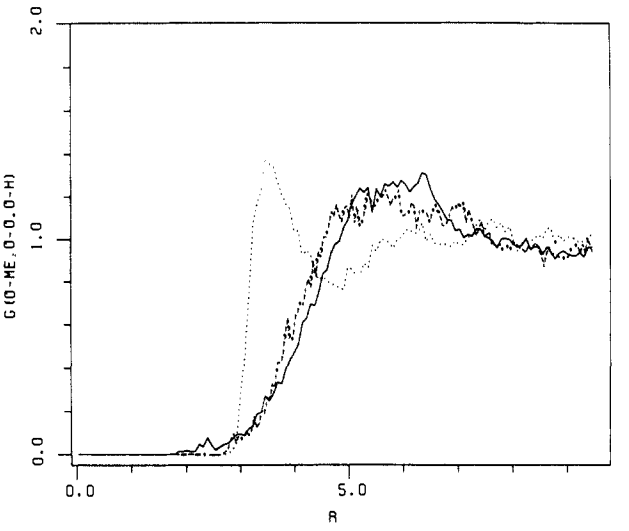


**Figure 8.** $T_1$ excited-state acetone–methanol site–site radial distribution functions. Line key is same as in Figure 6.

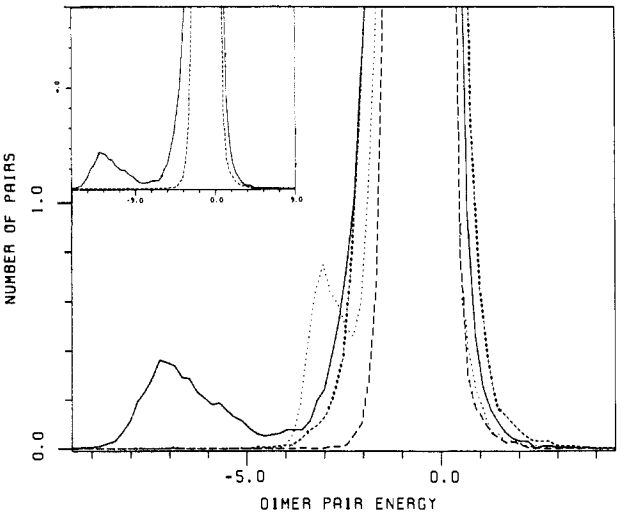


**Figure 9.** Acetone–methanol dimer pair energy distribution functions: equilibrated ground state, solid line; Franck-Condon $T_1$ excited state, dots; equilibrated $T_1$ excited state, longest dashes; Franck-Condon emission state, short dashes. Inset: methanol–methanol distribution function, light line; others are the same as above.

decrease in the series ground-state acetone, methanol, excited-state acetone. The Franck-Condon excited-state acetone (dotted in main plot) benefits energetically from the optimally oriented methanol solvent shell. Some weak hydrogen bonding (about −3 kcal/mol) is in evidence (also see Table IV), as well as general solute–solvent electrostatic interactions that are more favorable than those after excited-state equilibration. As would be expected on consideration of the near-shell solvent configuration about the equilibrated excited-state acetone, very little recovery of electrostatic interactions occurs at the Franck-Condon emission state in methanol (short dashes); only 0.18 worth of a hydrogen bond is indicated (Table IV).

From the viewpoint of a polar solvent, acetone appears hydrophobic in its $\pi^*$ excited state relative to the ground state. We have demonstrated how the solute–solvent potential energy of interaction becomes progressively less favorable on excitation and equilibration of the Franck-Condon excited state. We have also reasoned that we expect near-shell solvent–solvent potential energy of interaction to grow more favorable on equilibration of the Franck-Condon excited state. A plot of solvent–solvent energy as a function of radial distance out from the center of mass of the solute to the center of mass of the methanol solvent molecules (Figure 10) shows that near-shell methanol solvent–solvent potential energy of interaction is indeed stronger when the excited state (solid line) is being solvated. Note that the average potential

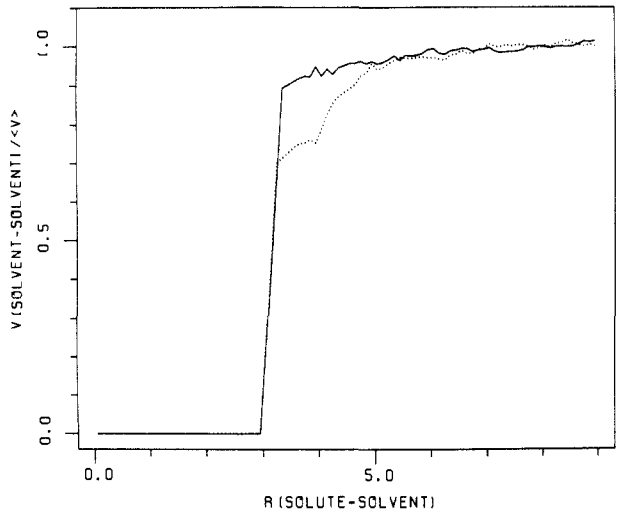


**Figure 10.** Acetone–methanol solvent–solvent potential energy of interaction (normalized) as a function of radial distance out from the center of mass of the solute: equilibrated ground state, dots (average over 3300 configurations); equilibrated $T_1$ excited state, solid line (average over 3000 configurations). $R$ is in angstroms.

energy of solvent–solvent interaction is attained (where $V/\langle V\rangle$ approaches 1.0) at a radial location nearer to the excited acetone than for the ground-state acetone, illustrating (as has already been discussed) the change in the nature of near-shell solvent–solvent interactions. This also indicates that a more rigid solvent "cage" structure forms around the more hydrophobic form (excited state) of the solute acetone in methanol. A similar though less pronounced result (plot not shown) was calculated for acetone in water solvent.

## Summary and Conclusion

Calculations using a molecular dynamics implementation of the statistical mechanical perturbation method have satisfactorily reproduced the spectroscopically observed trend for the shifting of an alkyl carbonyl compound's n $\rightarrow \pi^*$ transition frequency further toward the blue in progressively more polar solvents. We found that simple point charge modeling of the electronic distributions in the ground and excited states of the solutes acetone and formaldehyde and the use of a classical two-body potential energy function enabled the nearly quantitative determination of shift energies when the predominant solute–solvent interactions were due to non-induced electrostatics (as when these solute excitations were considered in water). This further validates our approach to the development of charge models for molecular mechanical/dynamical simulations of molecules.[21b]

Where previous researchers have studied hydrogen bonding orientation and energetics for these solute–solvent interactions using ab initio methods which considered isolated vapor-phase dimers or clusters,[11a,b] and determined that this approach is inadequate for studying solvent spectral shifts,[34a] we have investigated these issues within the context of "infinite" solvation (using a variety of solvents), where many explicit solvent molecules interact simultaneously with the (ground or excited state) solute of interest. This led to reasonable quantitations of the numbers of hydrogen bonds formed, their strengths, and orientational behaviors where the ground-state, Franck-Condon states, and thermally equilibrated excited-state solutes were examined. We were able to illuminate the relation of solvent restructuring around the excited-state solute to the differential solvation of ground and excited states and demonstrated that less-polar Franck-Condon excited-state solutes are actually further desolvated during thermal equilibration in polar solvents. This result concurs with and extends Haberfield's[12] experiments which demonstrated that when a carbonyl solute is transferred from a nonpolar to a polar hydrogen-bonding solvent, the blue shift of the n $\rightarrow \pi^*$ band is due not only to superior solvation of the ground state but also in substantial part to the desolvation of the excited state in the polar solvent. A key realization here is that simple ketone groups's excited-state charge distributions render them hydrophobic compared to the ground-state solutes and that their mainly nonpolar character encourages the optimization of solvent–solvent interactions in polar solvents such as water and methanol.

Using this approach, we were unable to reproduce the red shift of acetone's n $\rightarrow \pi^*$ absorption band in the nonpolar solvent $CCl_4$. The rationale for this involves the neglect of explicit polarizability in the solvent and solute models. It warrants comment that although the effects of differential dispersion interactions and polarizability-mediated electro-inductive energies are expected to be relatively small in most perturbation calculations, they may contribute significantly in specific situations; the case of n $\rightarrow \pi^*$ shifts in nonpolar solvents is a case in point. Inclusion of these terms in an accurate way is likely to require either a quantum dynamical treatment or quantum mechanical–molecular mechanical coupling,[34] where the diffuse nature of the excited-state solute can be accounted for, and solvent polarizability is explicitly considered. When differential dispersion interactions between ground and excited states with the solvent contribute heavily to a red shift, the effect could also probably be reproduced empirically, at least in part (albeit somewhat crudely), by using a simple point charge model along with specifically fit van der Waals potential parameters $R^*$ (or $\sigma$) and $\epsilon$, which are nonidentical for the ground and excited states of the solute. The difference in transition-dipole formation energy might also be estimated from Bayliss's formula[10a] and added as a correction.

Further research, such as presented here for small solutes, which gives a qualitative, or even semiquantitative, description of solvation energetics and structure can naturally be extended to interesting and useful analyses of environmental effects on the electronic excitations of biologically important chromophores.[35]

**Acknowledgment.** We are glad to acknowledge research support from the National Science Foundation (CHE-85-10066). We thank Ronald Levy for his critical and helpful comments on the manuscript and for sharing copies of reprints (and preprints) of studies that he is involved in which were relevant to our work here. We are also grateful to Martin Shetlar, David A. Pearlman (especially for the use of his convenient plotting program), David Spellmeyer, and Piotr Cieplak for useful discussions.

(35) (a) Warshel, A. *J. Phys. Chem.* **1979**, *83*, 1640. (b) Warshel, A.; Weiss, R. M. *J. Am. Chem. Soc.* **1980**, *102*, 6218; **1981**, *103*, 446.